

WRINKLE INITIATION AND DEVELOPMENT IN HEATED WEBS ON DRUMS

By

Dilwyn P. Jones¹, Michael J. McCann², Charles A. Bishop³,
and Steven Abbott⁴

¹Emral Ltd., UK

²MJMcCann Consulting, USA

³C. A. Bishop Consulting Ltd., UK

⁴Steven Abbott TCNF Ltd., UK

ABSTRACT

Wrinkles often occur in webs heated on drums and rollers. Anecdotal evidence from vacuum metalizers suggests that wrinkles are initiated by small grit particles or surface imperfections that lift the web off the drum. An elliptical patch of web centered on the dirt particle is lifted off the drum against the tension pressure acting to restore contact. A numerical “tent model”, based on plate theory, has been formulated to predict the critical transverse direction (TD) stress at which the web spontaneously lifts off the grit, forming the wrinkle. The model iterates to find the tent shape for a given TD stress, and then uses an interval halving method to determine the critical TD stress. Results from the model will be presented. It turns out that a simpler, analytical “draped beam” model gives similar dependence on parameters but over-predicts the value.

Once a wrinkle initiates, it may grow to a size where it is more visible, but has limited length and is restrained against further growth. Further increase in compression enables it to grow by relieving the TD compressive stress in both the lifted-off region and the neighboring web still in contact with the drum. It will also extend in the machine direction (MD). In vacuum coating, wrinkling causes a loss in thermal contact with the cooled drum, the web heats up, expands and the wrinkle grows catastrophically.

NOMENCLATURE

A_{kb} , A	Matrix of coefficients in difference equations
B_b , B	Vector of constants in difference equations
B	Also, constant of integration
D	Plate stiffness of web (equation 2)
E	Young’s modulus of the web
f	User-specified convergence condition
h	Web thickness
i	Index for mesh point in the x direction
j	Index for mesh point in the y direction

k	Index for mesh point combining x and y : $k = i(n+1) + j$
k	Also, draped beam wavenumber, $k^2 = -N_y/D$
	Index for mesh point under test for lift-off
l	Mesh point index (as k)
l	Also, half-length of draped beam.
m	Index i at the edge of the rectangular region in the tent model
M	Index i at the boundary of the lift-off region along the x -axis
MD	Machine Direction, i.e. along direction of travel
n	Index j at the edge of the rectangular region in the tent model
N_x	Tensile force per unit length acting in the MD
N_y	Tensile force per unit length acting in the TD
N_l	Lower bound on solution to critical TD load
N_u	Upper bound on solution to critical TD load
q	Contact pressure of drum surface acting on web
r	Ratio of squared MD and TD mesh spacings α^2/β^2
R	Drum radius
TD	Transverse Direction, i.e. perpendicular to direction of travel
w	Displacement of web above the roller surface
\tilde{w}	Dimensionless displacement = w/w_0
w_0	Web displacement at origin, equal to grit height
w_{ij}	Web displacement at mesh point i,j
x	MD coordinate
y	TD coordinate
α	MD mesh spacing
β	TD mesh spacing
ν	Poisson's ratio of web
∇^4	4 th order partial differential operator (equation 3)

INTRODUCTION

Webs are frequently heated on drums and rollers, where thermal expansion attempts to reduce tension and increase the web width. Frictional forces between the web and drum surface restrict the width increase, instead causing a transverse direction (TD) compressive stress. This may cause buckling of the web into one or more wrinkles, lifting it off the drum surface [1]. Many hot thermoplastic webs are soft and retain permanent memory of the wrinkle deformation after cooling, resulting in unsatisfactory product. However, in vacuum coating where the web is heated by radiation and deposition of vapor, its temperature continues to rise when thermal contact between the cooled drum and web is lost under the wrinkle. The substrate heats up further and expands, resulting in runaway wrinkle growth.

Anecdotal evidence from vacuum metalizers suggests that wrinkles are initiated by small grit or dirt particles or surface imperfections that raise the web off the drum [2,3]. An oval patch of web centered on the grit particle lifts off the drum against the tension pressure acting to restore contact, forming a "tent". As the TD compressive stress grows, the contact force on the grit falls until it reaches zero. This is a point of instability, as a small upward displacement requires negative contact force to maintain equilibrium. In the absence of adhesion, contact pressure cannot be negative, so the tent grows spontaneously. This is taken as the initiation of a wrinkle.

A numerical “tent model”, based on plate theory, has been formulated to predict the critical TD stress. It iterates to find the tent area and shape for a given TD stress, and then uses an interval halving method to determine the critical TD stress. The model and results from it are described below. It turns out that a simpler, analytical “draped beam” model [3] gives similar dependence on parameters but over-predicts the critical value by 28 to 32%. This is also outlined in the paper, along with its implementation in web handling simulation software.

The issue of what happens to a wrinkle once initiated is discussed, and compared with observations.

WRINKLE INITIATION

A web under machine direction (MD) tension wrapping a cylindrical drum or roller exerts a “tension pressure” on it, similar to the tension in a rubber balloon skin balancing the gas pressure inside. The web experiences an equal and opposite reaction, the contact pressure. Practical drum surfaces are not perfectly smooth at the microscopic level, but carry occasional grit (contamination) particles and have a topography with local peaks. An isolated grit particle or large peak will lift an oval-shaped region of the web off the drum, but outside the region, the web will remain in contact (figure 1). There will still be a contact pressure outside the region, but it will be zero inside the region, apart from a high value acting over the very small area of contact with the grit.

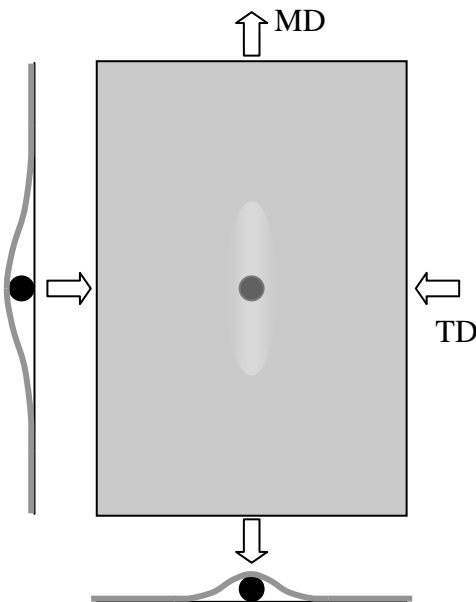


Figure 1 – Sketch of grit particle creating an oval tent in the web. Arrows show the stresses acting.

As TD compressive stress in the web is raised from zero (e.g. by temperature rise), the contact force on the grit falls, until at a critical TD stress it becomes zero. Further increase in TD stress causes a negative contact force, i.e. drum, grit and web must be attached by some sort of adhesive force, or the web will lift off. The critical TD stress

falls with increasing grit particle size, so represents instability: the web will lift off the grit once the critical value is exceeded. This “tent model” has been formulated to find the critical TD stress numerically.

Tent Model Theory

MD and TD stresses are assumed to be constant in the small patch of web under consideration, generally smaller than 20 mm. Shear stresses and friction forces are absent. The grit particle is assumed to be small enough so that deformations are due to bending only, with no change in MD or TD stress.

The web is treated as plate, subjected to loads normal to the surface and in the plane, as shown in figure 2. Displacement w is measured outward from the drum surface, radius R . Curvilinear coordinates (x,y) are taken in the MD and TD directions respectively. The web obeys the 4th order partial differential equation [4,5]:

$$D\nabla^4 w - N_x \frac{\partial^2 w}{\partial x^2} - N_y \frac{\partial^2 w}{\partial y^2} + \frac{Ehw}{R^2(1-\nu^2)} = q - \frac{N_x}{R} \quad \{1\}$$

The plate stiffness D is given by:

$$D = \frac{Eh^3}{12(1-\nu^2)} \quad \{2\}$$

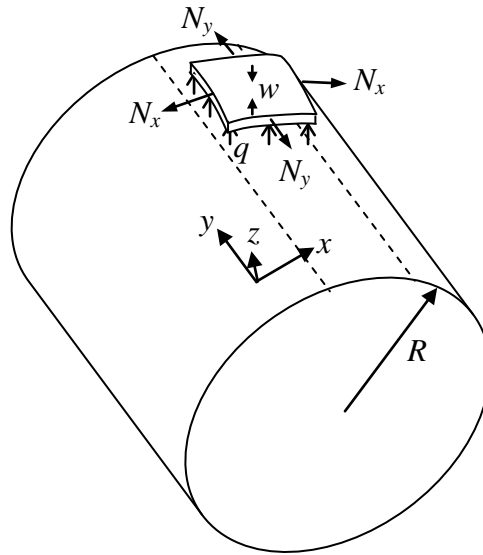


Figure 2 – Small element of web on drum showing coordinate system, in-plane loads N_x , N_y and contact pressure q acting.

N_x and N_y are the in-plane loads (tensile force per unit length, or stress integrated over the thickness in the MD and TD respectively); E and h the Young’s modulus and thickness; ν is Poisson’s ratio; and q the contact pressure at each point (x,y) . When the web rests on the drum surface, $w = 0$, and the tension pressure is balanced by contact

pressure, i.e. $q = N_x / R$, except at the boundary of the lift-off region. At the grit particle, the displacement is specified as w_0 .

At the boundary line between the portions in and out of contact, the displacement, slope and curvature are zero both normal and tangential to the line.

Finite Difference Equations

The differential equation is solved numerically on a rectangular grid, with indices i, j and intervals α, β in x, y respectively. The finite difference approximations are:

$$\begin{aligned} \left(\frac{\partial^2 w}{\partial x^2} \right)_{i,j} &= \frac{w_{i-1,j} - 2w_{i,j} + w_{i+1,j}}{2\alpha^2} \\ \left(\frac{\partial^2 w}{\partial y^2} \right)_{i,j} &= \frac{w_{i,j-1} - 2w_{i,j} + w_{i,j+1}}{2\beta^2} \end{aligned} \quad \{3\}$$

$$\begin{aligned} (\nabla^4 w)_{i,j} &= \left(\frac{\partial^4 w}{\partial x^4} + \frac{\partial^4 w}{\partial y^4} + 2 \frac{\partial^4 w}{\partial x^2 \partial y^2} \right)_{i,j} \\ &= \frac{1}{\alpha^2 \beta^2} \left[\begin{aligned} &(6/r + 6r + 8)w_{i,j} + 1/r(w_{i-2,j} + w_{i+2,j}) - (4/r + 4)(w_{i-1,j} + w_{i+1,j}) \\ &+ r(w_{i,j-2} + w_{i,j+2}) - (4r + 4)(w_{i,j-1} + w_{i,j+1}) \\ &+ 2(w_{i-1,j-1} + w_{i+1,j-1} + w_{i-1,j+1} + w_{i+1,j+1}) \end{aligned} \right] \end{aligned}$$

where $r = \alpha^2 / \beta^2$.

The grit particle is located at (0,0). Symmetry is invoked, leading to the choice of a rectangular mesh in the first quadrant. The symmetry boundaries are dealt with by substituting for displacements at points lying at x or $y < 0$:

$$w_{i,j} = w_{-i,j} = w_{i,-j} = w_{-i,-j} \quad \{4\}$$

Writing out all the finite difference equations, multiplied by $\alpha^2 \beta^2 / D$, and using dimensionless displacement $\tilde{w} = w / w_0$ and the new label $k = i(n+1) + j$ for each point, leads to the matrix equation:

$$A_{kl} \tilde{w}_l = B_k \quad \{5\}$$

Each point k that has lifted off at any stage in the solution generates several elements in row k of the matrix A , and

$$B_k = -\frac{N_x \alpha^2 \beta^2}{DR w_0} \quad \{6\}$$

Points still in contact have $B_k = 0$ together with $A_{kl} = 1$ if $l = k$, or $A_{kl} = 0$ for l not equal to k . Mesh points in the rectangular region from the origin to points m and n in x and y are capable of lifting off. Points lying outside have zero displacement, therefore

terms such as $A_{k,n+1}$, $A_{k,n+2}$, $A_{m+1,l}$ and $A_{m+2,l}$ do not arise in the equations. However, their contact pressure can still be calculated.

Solution of the matrix equation gives the shape of the “tent” for the current imposed MD and TD loads and lifted-off region. Location of the boundary line is a little trickier. If it cuts the x -axis at $i=M$, expressing the conditions of zero displacement, slope and curvature with finite differences leads to $w_M = w_{M-1} = 0$, and the last non-zero value is w_{M-2} . Therefore, the boundary is located one interval further away from the origin than the first point with zero displacement. No attempt has been made to locate the boundary line away from the x and y axes.

Iteration Scheme

Neither the indices of the points in the lifted-off region nor the critical TD load are known initially, so these must be found in the solution process. This uses two loops as shown in figure 3: an inner loop to determine the points lifted off for a particular TD load, and an outer loop to determine the critical value. The first value of TD load is chosen to be the result of a one-dimensional beam model (equation 11 below). This is known to be an underestimate of the true critical value, so is taken as an upper bound N_u . Each initial run of the inner loop assumes the same rectangular subregion based at the origin within the m by n mesh to be lifted off, i.e. have zero contact pressure.

Inner loop. After each solution of the matrix equation, the contact pressure at all points in the region $(m+1, n+1)$ is calculated. If the lowest value is significantly less than zero, the web is trying to lift off at that point. If it is less than the test value of fN_x/R , then point k' where it occurs is lifted off: the matrix elements $A_{k',l}$ and $B_{k'}$ are recalculated, and the matrix equation solved again in the next pass through the inner loop. f is a user-specified convergence factor, typically 0.001. Points are thus lifted off one by one and displacements and pressures recalculated after each pass. The inner loop is stopped once there are no negative contact pressures larger than the test value.

The inner loop is run to completion if the contact pressure at the origin remains positive, but if it becomes negative the loop is terminated and the next value of N_y used, unless the step is to be the final one.

Outer loop. After convergence of the inner loop, the contact force at the origin is calculated. If positive, the upper bound on the critical value, N_u , is set equal to the current N_y . Otherwise, the lower bound N_l is set instead (note that the critical stress and the bounds are all negative). After the first pass through the outer loop, N_y is doubled for the next pass, then trebled, etc until a lower bound is found. Once both bounds have been found, the next value of N_y is taken as their average. The process continues until convergence is achieved, judged by the ratio $N_l / N_u < 1+f$.

Implementation

The model is programmed in VBA as part of a Microsoft Excel® workbook. The matrix equation is solved with the routine RMatrixSolve from the Alglib library [6]. In order to reach a solution in a few minutes at most on a low specification PC, meshes 10 by 10 or smaller are used, with around a quarter of points lifted off initially. Choice of mesh spacing is based on one-dimensional solutions for beams under lateral load and either axial tension or buckling under compression.

Checks for any negative displacements and contact pressures are included. If detected, the program ends with a message suggesting that the user should retry with fewer points lifted off initially or a different mesh size respectively.

Undoubtedly, further work could lead to more automation in setting up the problem and less risk of an aborted solution.

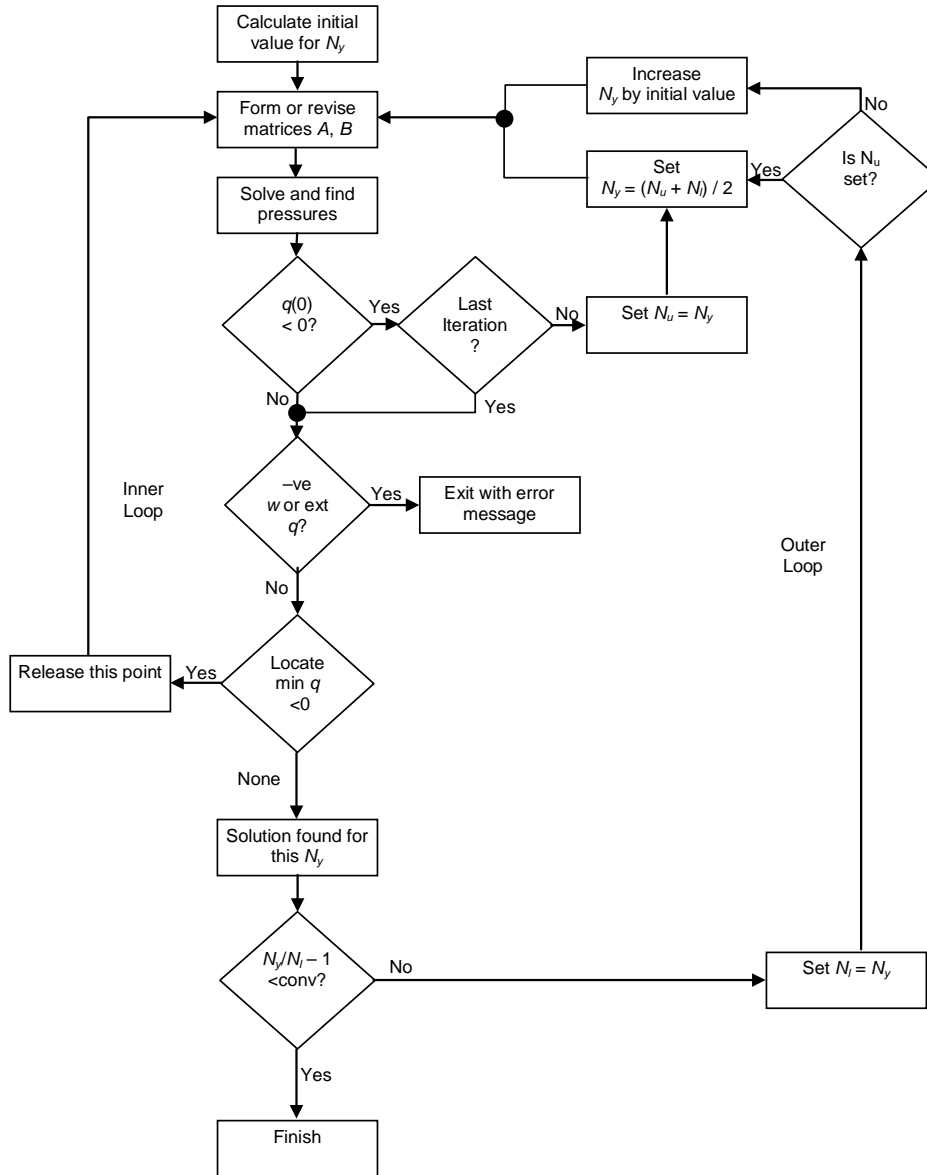


Figure 3 – Tent Model Flowchart

Output

The program tabulates displacements and contact pressures throughout the solution region. Numerical values of the critical N_y and the semi-axis lengths of the oval region are also output.

Parametric Study

Base Case. The model was run for a typical case before exploring the effect of varying parameters. The base values, which give a notional web strain (stress divided by Young’s modulus) of 0.1%, are given in Table 1:

Parameter	Symbol	Unit	Base Case	Range
Young’s Modulus	E	GPa	4	0.5 - 10
Poisson’s Ratio	ν	0.3	0.3	0.2 - 0.5
Thickness	h	μm	25	5 - 50
Drum Radius	R	m	0.5	0.1 - 1.1
Grit height	w_0	μm	1	1 - 10
Tension	N_x	N/m	100	50 - 300
MD step length	α	mm	0.25	
TD step length	β	mm	0.1	
Mesh size	m,n		8 by 8	

Table 1 – Model input for the Base Case and Parametric Study.

The model predicts a critical TD load of 182 N/m. This corresponds to a compressive strain of 0.18%, on top of the Poisson contraction of 0.03%.

The predicted shape of the “tent” at the point of instability is shown in figure 4. An oval area 4.5 by 1.8 mm lifts off, giving an aspect ration of 2.5.

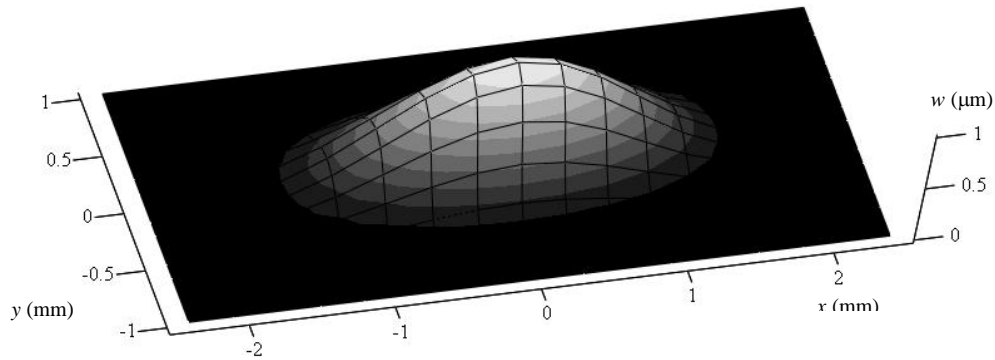


Figure 4 – Plot of displacement for Base Case.

The coarseness of the mesh results in an uncertainty in the area lifted off: the axes could be in error by double the step length (0.5 by 0.2 mm). This was borne out by a mesh refinement study. However, the total range of critical load was only 1.4% with various mesh sizes from 6 to 12 in x and y . Hence, the prediction of critical load is only weakly dependent on the mesh.

Effect of grit size. The effect of defect size on critical TD load is shown in figure 5 for different tensions. As expected, the critical load decreases with increasing grit size.

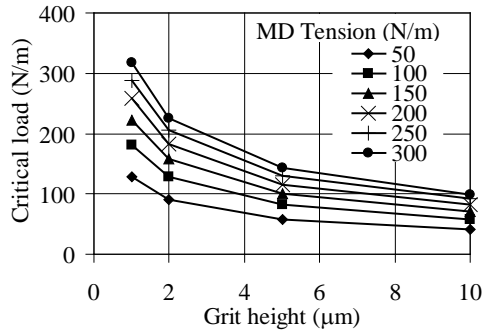


Figure 5 – Effect of grit height on critical load for different MD tensions.

Effect of MD Tension. The same points are replotted in figure 6 to show the increase in critical TD load with MD tension.

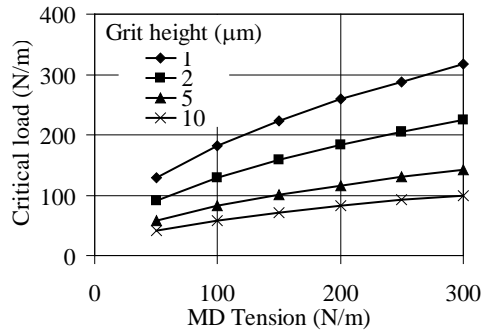


Figure 6 – Effect of MD Tension on critical TD load for different grit heights.

Effect of web properties. Figure 7 shows that the increase in critical TD load is linear with modulus at constant notional web strain (0.1%). This is unsurprising, as the differential equation is linear and solutions are unchanged when all coefficients are multiplied by the same factor, i.e. loads are increased in proportion to modulus.

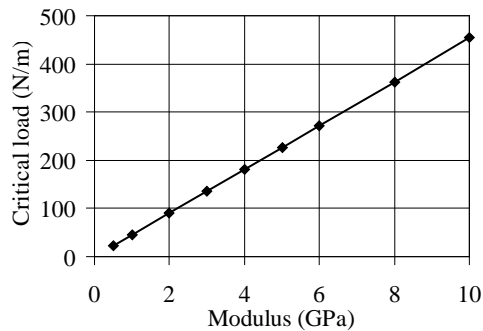


Figure 7 – Effect of web modulus on critical load at constant notional MD strain of 0.1%

Increasing Poisson's ratio from 0 to 0.5 increases the buckling load from 173 to 200 N/m, a small change. This result suggests that foams materials will be slightly more prone to wrinkling, and rubbery materials less so, as a result of their Poisson's ratio.

Effect of web thickness. The critical TD load depends strongly on web thickness, as shown in figure 8. The load is proportional to the square of thickness at constant notional web strain, and therefore linear with thickness at constant MD tension.

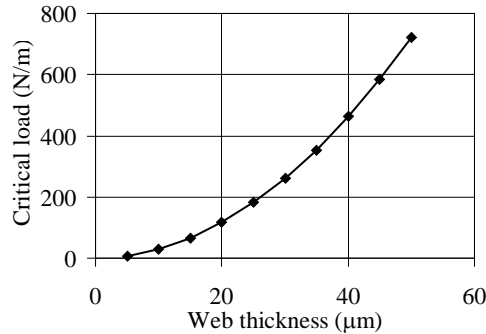


Figure 8 – Effect of web thickness on critical TD load at constant web strain of 0.1%.

Normal guidance for web handling and winding tension is to maintain constant web strain as thickness is reduced. This will result in greater wrinkling tendency for thinner webs. If instead the linear tension is kept constant, the critical TD load decreases linearly with thickness. This corresponds to a constant TD compressive strain, which may arise from a temperature rise independent of thickness.

Effect of drum size. The effect of drum radius is shown in figure 9. The tension pressure is greater for a smaller radius, and hence the critical TD load is higher. Larger drums may be designed to give more length for deposition and heat removal, but this could be at the expense of a stronger wrinkling tendency.

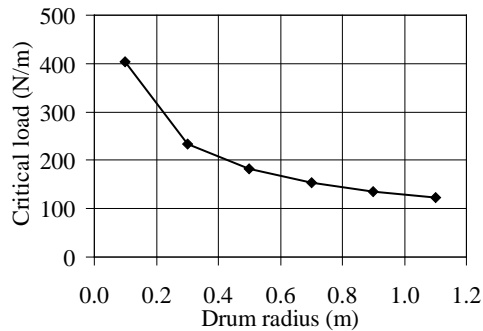


Figure 9 – Effect of drum radius on critical TD load.

Aspect Ratio. The ratio of MD to TD axis length in the lifted off region varies from 2.4 to 5 for the conditions examined. It increases with MD tension, grit size, drum radius

and decreasing web thickness (at fixed notional web strain). Modulus and Poisson's ratio have little effect.

Draped Beam Model

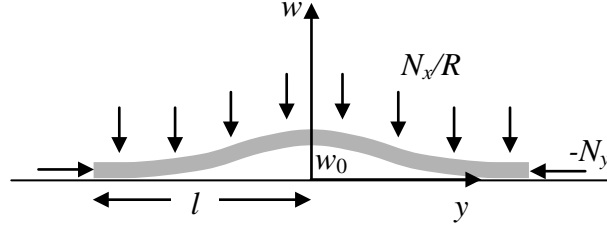


Figure 10 – Draped beam model at the point of lifting off the grit, showing axial compressive force $-N_y$ and tension pressure N_x/R acting.

An alternative to the tent model has been developed based on beam theory. The web is locally held off the drum by the particle of grit, height w_0 , and is pressed towards the drum by tension pressure equal to N_x/R only. At the point of instability, the contact pressure q is zero along the whole length, including the point of contact with the grit. Contributions from bending in the machine direction and extra MD stretch are neglected. With these approximations, equation 1 becomes the equation for a beam with length $2l$ in the TD as shown in figure 10:

$$D \frac{d^4 w}{dy^4} - N_y \frac{d^2 w}{dy^2} = -\frac{N_x}{R} \quad \{7\}$$

The solution is symmetric in y and has the form

$$w = A \cos ky + By^2 + C \quad \{8\}$$

Substituting into equation 7 gives:

$$\begin{aligned} k^2 &= -N_y/D \\ B &= N_x/2RN_y \end{aligned} \quad \{9\}$$

At the ends of the beam, the boundary conditions $dw/dy = 0$ and $d^2w/dy^2 = 0$ lead to the transcendental equation:

$$\tan kl = kl \quad \{10\}$$

$$N_y = -\sqrt{\frac{DN_x}{Rw_0}} \sqrt{1 + \frac{1}{2}(kl)^2 - \sec kl} = -3.96 \sqrt{\frac{DN_x}{Rw_0}} \quad \{11\}$$

The length of the beam is given by:

$$2l = 4.51 \sqrt[4]{DRw_0/N_x} \quad \{12\}$$

These results can also be obtained by superposing standard solutions for beams under combined axial compression and transverse loading, for example from [7].

Comparison with tent model. For the cases presented in figures 5 to 9, the draped beam model predicts a critical TD load a factor 1.28 to 1.32 smaller than the numerical model. It is smaller because the extra restoring forces of bending in the MD and lift-off causing MD stretch are ignored. It is quite surprising that the ratio of the two predictions is nearly constant.

The beam length ranges from just below to 10% above the numerical model prediction of the TD width of the area lifted off. Part of the variability is due to the effect of the discrete mesh in the tent model, as noted above. However, it appears that the 95% of the draped beam value is a good estimate of the numerical model result.

Comparison with classical shell buckling theory

An end loaded cylindrical shell is predicted to buckle when the TD load reaches [8]:

$$N_y = -\frac{Eh^2}{R\sqrt{3(1-\nu^2)}} \quad \{13\}$$

This is generally one to two orders of magnitude lower than the predictions of either the tent or draped beam model. For example, the conditions plotted in figures 5 and 6 all give the same predicted shell buckling load in equation 13 of 3.0 N/m.

The classical expression is unrealistic, as it does not account for the stabilizing effect of the tension pressure pushing the web against the rigid roller.

WRINKLE DEVELOPMENT

Observations

The onset and development of wrinkling on vacuum metalizing drums has not been the subject of dedicated experimental measurements. However, it appears that raising the heat input does make the web more susceptible to wrinkling. As its temperature increases, the compressive TD stress increases and hence the critical value is exceeded for smaller grit particles or defects.

The deposition process becomes impossible to run if wrinkles initiate, grow and hence become permanent. However, there is an intermediate regime where short wrinkles appear at random locations on the web. They are visible as elongated “tents”. Once they reach the drum exit point, they disappear. They do not reappear at the same location one drum revolution later, suggesting they are initiated by a temporary defect such as grit, rather than a surface asperity on the drum.

Tent and Draped Beam Model Predictions

Both models predict that the web is distorted as it covers a grit particle. Even under zero TD load, the tent shape is not very different from that at instability, and certainly the height is the same.

Once the critical TD load is exceeded slightly, the tent becomes unstable and increases in height and area. The draped beam model exhibits similar behavior, and predicts a second equilibrium configuration at the next solution of equation 10. where the beam is 1.7 times longer, and the shape has a double peak with height 2.2 times greater. It is likely that an extension of the tent model would also predict equilibrium positions above the original grit height.

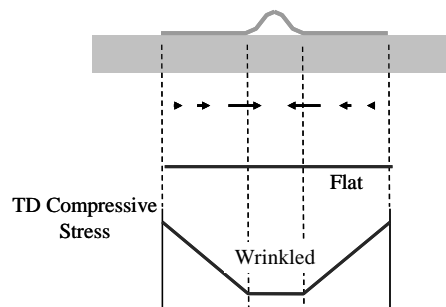
It is possible that when a short wrinkle is observed, the web is in this second equilibrium position; in other words, it has lifted off the initiating grit particle. This makes the wrinkle higher and easier to see. It also explains why the appearance of the short wrinkles is not reported when the web wraps the drum without heat load, even though it still rests on all the grit particles.

It would be interesting to explore the tent model further by calculating the negative contact force on the peak as its height is increased whilst maintaining the TD load at the critical value. The existence of a second equilibrium position would lend support to the idea the short wrinkles lift off the initiating grit particles.

Further growth of wrinkles

As the heat load increases, wrinkles on a drum extend for a considerable distance in the MD, form with appreciable TD separation, and are long-lived. An additional mechanism for wrinkle growth is believed to come into effect, where the TD stress is relieved as the wrinkle rises away from the surface [9,10]. Friction acts laterally on the web as it slips towards the wrinkle, giving a stress gradient and relieving strain energy in both the lifted-off region and the neighboring web still in contact with the drum. As the wrinkle grows, it also loses compressive strain energy but gains bending strain energy. Eventually, a condition of minimum energy is reached, determining wrinkle geometry.

An earlier model by the authors for energy in the wrinkled web [10] is being extended to include work done against friction during wrinkle growth. The variation of strain energy with wrinkle width, height, and TD stress relief should lead to predictions of their values and regions of stability. Some progress has been made, and it is hoped to report the work at a later conference. As before, one or more discrete wrinkles in the MD form across the width, each surrounded by a zone where the web has slipped sideways to feed material into the wrinkle (figure 11). The new model should be useful in understanding the wrinkle patterns observed.



If the development of TD compression is affected by contact between the web and drum, the wrinkle development may be accelerated or retarded. For example, in vacuum deposition, the area of web that initially lifts off will heat up more rapidly as thermal contact with the cooling drum is reduced. This will increase the TD compressive stress from thermal expansion effects, and rapidly lead to a runaway effect. On the other hand, web on a heating roll may cool down as it leaves the surface, inhibiting further growth.

APPLICATION

MD and TD stresses in a web on a drum vary with position when it is attempting to change length because of thermal expansion, moisture or solvent concentration changes, viscoelastic relaxation or other causes. This becomes complex when microslip occurs as a result of insufficient friction to sustain large stress gradients. An earlier paper analyzed steady-state stress variation on heating and cooling rollers, and during vapor deposition [11]. The MD and TD stresses were calculated at all points around the drum.

This stress calculation has been incorporated in the software package TopWeb2 [12] as an optional extra for vacuum deposition. It includes the draped beam criterion for wrinkle initiation (equation 11), considering whether the TD stress exceeds the critical value at all points on the drum. The user must input the grit height, and an initial value for TD strain coming onto the drum in order to take account of prior spreading or troughing. If the tent model is considered to be more accurate, the draped beam model prediction is conservative. A safety factor gives a guide to the risk of wrinkling if conditions deviate from the assumed values. It is then possible to use the software to simulate the effect of material properties, deposition process settings, drum temperature and dimensions, line speed and tension settings on the likelihood of wrinkling [3].

CONCLUSIONS

A realistic numerical model for wrinkle initiation on a drum or roller has been developed. A pre-existing grit particle or surface defects holds the web off the surface in an oval-base tent shape. As TD load increases, for example from thermal stresses, a critical point is reached when the contact force on the grit drops to zero. Beyond this, the web lifts off further. The critical TD load is higher for larger MD tension, modulus, thickness and Poisson's ratio, and for smaller grit size and drum radius.

A simpler, analytical draped beam model seems to capture the same behavior quite well, giving predictions around 75% of the numerical model. It has been applied in commercial web handling software as part of a vacuum deposition simulation, where the web heats up, changes stress and develops a tendency to wrinkle.

Both models should be regarded as approximations. Conditions on any line and material properties vary with time, so a safety factor approach is appropriate. An additional complication is the disturbance caused to the web by the changed thermal contact around the grit particle, both before and after wrinkle initiation.

Development of the wrinkle into something observable and possibly damaging occurs once the critical TD load is exceeded. The draped beam model suggests that there is a second equilibrium position, where the wrinkle has lifted off the initiating grit particle but only in its immediate vicinity. This may correspond to the "short wrinkles" reported before catastrophic wrinkling sets in at higher heat input. Beyond this point, the main driving force is the relief of TD compressive stress reducing the overall strain energy. This occurs not only by the extra width developed in the curved wrinkle cross-section, but also by web feeding laterally into the wrinkle from either side.

REFERENCES

1. Shelton J. J., "Buckling of Webs from Lateral Compressive Forces", Proceedings of the Second International Conference on Web Handling. Ed. Good, J. K., Oklahoma State University, 1993.
2. McCann, M. J., Jones, D. P., and Affinito, J., "Buckling or Wrinkling of Thin Webs off a Drum," Society of Vacuum Coaters 47th Annual Technical Conference, 2004, pp. 638-643.
3. McCann, M. J., Abbott, S. J., Jones, D. P., and Bishop, C. A., "The Power of Simple Models Used on Complex Processes," Proceedings of the AIMCAL Fall Technical Conference. 2010.
4. Timoshenko, S. P. and Woinowsky-Krieger, S., Theory of Plates and Shells, McGraw-Hill, New York. 1987.
5. Ducotey, K. S. and Good, J. K., "A Numerical Algorithm for Determining the Traction Between a Web and a Circumferentially Grooved Roller," Journal of Tribology, Trans ASME, Vol.122, 2000, pp. 578-584.
6. ALGLIB (www.alglib.net), Sergey Bochkhanov and Vladimir Bystritsky.
7. Young, W. C. and Budynas, R. G., Roark's Formulas for Stress and Strain, 7th ed., McGraw Hill, New York, 2002.
8. Timoshenko, S. P. and Gere, J. M., Theory of Elastic Stability, McGraw Hill, New York, 1961.
9. Clow, H., "A Model for Thermal Creasing and its Application to Web Handling in Roll to Roll Vacuum Coaters," Society of Vacuum Coaters 32nd Annual Technical Conference, 1989, pp.100-103.
10. Jones, D. P. and McCann, M. J., "Wrinkling of Webs on Rollers and Drums," Proceedings of the Eighth International Conference on Web Handling, Ed. Good, J. K., Oklahoma State University, 2005, pp. 123-140.

12. Available from Rheologic Ltd, Leeds, UK. www.rheologic.co.uk.